Simulation of high efficiency bifacial solar cells on n-type substrate with AFORS-HET

WANG LISHENG*, CHEN FENGXIANG
Department of physics science and technology, Wuhan University of Technology, Wuhan city, Hubei province, P.R.China. 430070

Hetero-junctions of hydrogenated amorphous silicon and mono-crystalline silicon, a-Si:H/c-Si, are of technological interest in particular for highly efficient solar cells. Here the simulation and design of high efficiency bifacial solar cell on n-type substrate with AFORS-HET was presented. The influence and optimal results of the front contact, the back contact and the interface defect states were discussed. The computation result shows that the introduction of the intrinsic buffer layer between a-Si:H/c-Si hetero-junction is mainly used to decrease the interface states density. If D_{it} is lower than $10^{11}cm^{-3}$, the undoped a-Si:H(i) buffer layer can be cancelled at the expense of the conversion efficiency just one percent lower compared to standard HIT solar cells.

(Received December 6, 2010; accepted January 26, 2011)

Keywords: Hetero-junction solar cells, Interface defect states density, Work function, Simulation

1. Introduction

Silicon HIT (Hetero-junction with Intrinsic Thin-layer) solar cell is now attracting much interest, because very high efficiencies (above 22%) have been demonstrated and Sanyo has started the production of commercial photovoltaic HIT-modules [1]. Fabrication of HIT solar cells involves the deposition of thin intrinsic hydrogenated amorphous silicon layers on both sides of silicon wafer by PECVD at low temperatures. This process can realize excellent surface passivation and p-n junction formation simultaneously [2]. In the last years many European groups have started work in this direction which involved both research into the physical properties of the hetero-junction and the development of devices. Laboratory efficiencies have been reported of up to 19.8% [3]. While the discrepancy between the Sanyo's efficiency and European efficiency suggests that a further investigation is necessary to fully understand the factors that affect the performance of the HIT solar cells.

In this paper, a bifacial high efficient HIT solar cell was simulated and optimized with the AFORS-HET software. The influence of various parameters for the front and the back structures was discussed. It was found that the interface defect states density was one key parameter which affects the solar cell photovoltaic characteristics. Detailed analysis and the optimization results for bifacial hetero-junction solar cell on n-type substrate were provided.

2. The bifacial HIT solar cell structure

Fig. 1a shows a schematic diagram of the bifacial HIT solar cell with a-Si:H(i) film inserted between doped amorphous silicon layers and the c-Si substrate. Transparent conductive oxide (TCO) layers are deposited on both sides of the structure to achieve a low series resistance. In contrast to the standard HIT structure, another structure without intrinsic amorphous layers was shown in Fig.1b. This structure leads to minimization of the overall a-Si:H thickness and thereby maximization of the cell quantum efficiency without much reduction of the open-circuit voltage (V_{oc})[4].

In both HIT structures, the n-type mono-crystalline film with thickness 300um was used as substrate. In the simulation process, the light reflection of the front contact comes from the file ZnO-a-Si-c-Si-pyramid.ref, which was one default value in AFORS-HET. The back reflection was set to be 1. The illumination condition is AM 1.5 ($100mW/cm^2$), corresponding to the effective wavelength ranges from 0.3um to 1.1um. The other simulating parameters were listed in Table 1. During the computation, all the parameters were adopted as the setting values except for the specific declared ones.

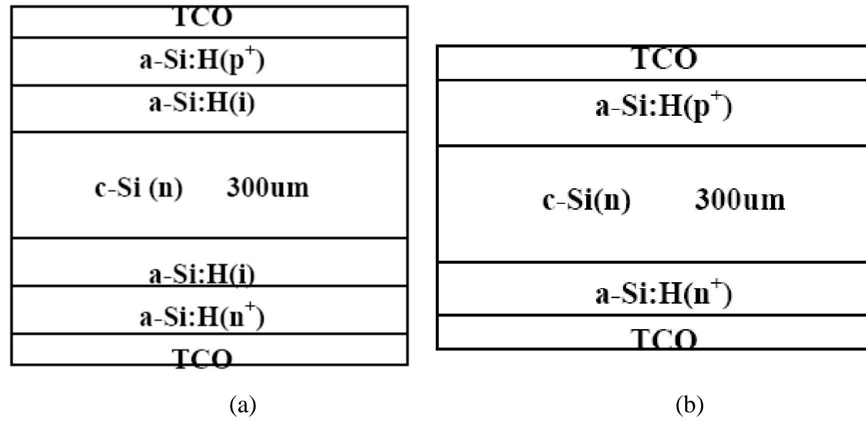

(a) (b)

Fig.1 The bifacial HIT structure used in the simulation: a) with an intrinsic thin amorphous layer and b) without it.

Table 1 The parameters adopted for the bifacial HIT solar cells.

	a-Si:H(p^+)	a-Si:H(i)	a-Si:H(n^+)	c-Si (n)
Thickness/nm	adjustable	adjustable	5	300000
Electron affinity/eV	3.8	3.8	3.8	4.05
Band gap /eV	1.8	1.8	1.8	1.12
Optical band gap/eV	1.72	1.72	1.72	1.12
N_c/cm^{-3}	$2.5\cdot10^{20}$	$2.5\cdot10^{20}$	$2.5\cdot10^{20}$	$2.8\cdot10^{19}$
N_v/cm^{-3}	$2.5\cdot10^{20}$	$2.5\cdot10^{20}$	$2.5\cdot10^{20}$	$1.04\cdot10^{19}$
Electron mobility /cm^{2}V^{-1}s^{-1}	10	20	10	1350
Hole mobility /cm^{2}V^{-1}s^{-1}	1	2	1	450
N_D/cm^{-3}	0	0	$1\cdot10^{19}$	$1.5\cdot10^{16}$
N_A/cm^{-3}	adjustable	0	0	0
Band tail density of states /cm^{-3}.eV^{-1}	$2\cdot10^{21}$	$2\cdot10^{21}$	$2\cdot10^{21}$	
E-Urbach/eV	0.06(E_D) 0.03(E_A)	0.06(E_D) 0.03(E_A)	0.06(E_D) 0.03(E_A)	
Capture cross-section for donor states,e,h /cm^2	$1\cdot10^{-15}$ $1\cdot10^{-17}$	$1\cdot10^{-15}$ $1\cdot10^{-17}$	$1\cdot10^{-15}$ $1\cdot10^{-17}$	
Capture cross-section for acceptor states,e,h /cm^2	$1\cdot10^{-17}$ $1\cdot10^{-15}$	$1\cdot10^{-17}$ $1\cdot10^{-15}$	$1\cdot10^{-17}$ $1\cdot10^{-15}$	
Gaussian density of states/cm^{-3}	$1\cdot10^{19}$	$8\cdot10^{16}$	$1\cdot10^{19}$	
Gaussian peak energy for donors, acceptors/eV	1.22, 0.70	1.22, 0.70	1.22, 0.70	
Standard deviation/eV	0.23	0.23	0.23	
Capture cross section for donor states,e,h/cm^2	$1\cdot10^{-14}$ $1\cdot10^{-15}$	$1\cdot10^{-14}$ $1\cdot10^{-15}$	$1\cdot10^{-14}$ $1\cdot10^{-15}$	
Capture cross section for acceptor states,e,h/cm^2	$1\cdot10^{-15}$ $1\cdot10^{-14}$	$1\cdot10^{-15}$ $1\cdot10^{-14}$	$1\cdot10^{-15}$ $1\cdot10^{-14}$	
O-vacancy density/cm^{-3}				$1.9\cdot10^{11}$

3. Simulation results and discussion

3.1 Optimization of the front contact

3.1.1 Influence of the emitter thickness

Fig. 2 shows the photovoltaic characteristics of the TCO/a-Si:H(p^+)/c-Si(n)/a-Si:H(n^+)/TCO cells varies with the emitter thickness. It can be seen from the Fig. 2, with the emitter thickness increases, the open circuit voltage keeps the same value; while the short-circuit current and the conversion efficiency decrease. According to ref. [5], a-Si: H amorphous film is a layer with high defect density, so carrier diffusion length in this layer is very short. Usually the photo-induced carriers in this layer were mainly driven by the high electric field strength across the whole layer and then collected and formed light current. When the thickness of amorphous layer increases, the electric field strength in the emitter will drop. It is easy to form "dead layer" (low field strength region) and then affect the transport and collection of photo-induced carriers. This is the main reason why the short-circuit current and efficiency decrease. But if the emitter is too thin, the hetero-junction is too shallow to influent by the existence of the interface states. Therefore the thickness of the emitter is selected at 5nm, corresponding to a sequence of about 20 Si-Si bonding lengths [6].

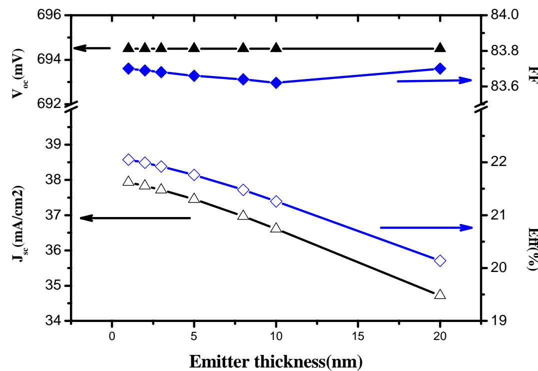

Fig. 2. The simulation I-V results for hetero-junction solar cell as a function of the emitter thickness.

3.1.2 The influence of the doping concentration of the a-Si:H(p^+) emitter

Fig.3 shows the effect of the p-type a-Si:H layer doping concentration on the performance of hetero-junction solar cell with the assumption that the TCO/a-Si:H(p^+) contact is a flat band. We can see that when N_A increases, the efficiency also increases, but above $2\times10^{19}cm^{-3}$ the solar cell efficiency is saturated and then decreases slowly, so that an optimal value of $2\times10^{19}cm^{-3}$ was chosen because a higher acceptor concentration than this is difficult to obtain in the laboratory [4]. According to the design principles for higher efficiency HIT solar cell [5], the low doping concentration in the emitter can avoid the appearance of the dead layer and is beneficial to the transport and collection of photo-induced carriers. But in order to increase the solar cell's open circuit voltage and reduce the series resistance, the doping concentrations of a-Si: H layer should be increase appropriately. While high doping concentration is accompanying with the appearance of the low electric field area, which requires further thinning of a-Si: H layer. Here $2\times10^{19}cm^{-3}$ is an optimum doping concentration, the corresponding efficiency is 21.77%.

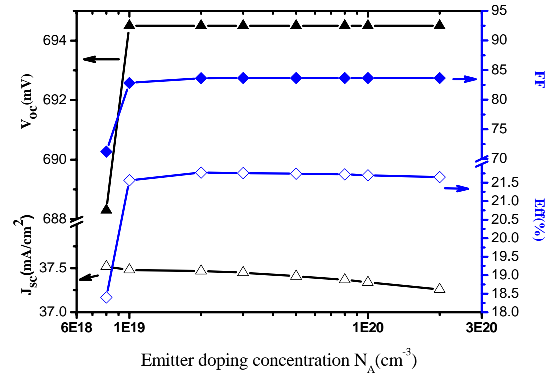

Fig. 3 The simulation I-V results for TCO/a-Si:H(p^+)/c-Si(n)/a-Si:H(n^+)/TCO solar cell as a function of the emitter doping concentration.

3.1.3 The influence of inserted intrinsic amorphous buffer layer and the interface states density D_{it}

3.1.3.1 An intrinsic buffer layer without interface states density was added.

In this section an intrinsic a-Si:H buffer layer is embedded between a-Si:H(p^+)/c-Si(n) hetero-junction structure. Though this structure was firstly developed by SANYO Company and this type solar cell was named as HIT solar cell, there is also a controversy on the need of such an intrinsic buffer layer. Some authors claim that it is beneficial, while others get good results without it and do not see significant improvements if they introduce it [1]. One reasonable explanation for the benefit of this undoped buffer layer is that the density of states in undoped a-Si:H is weaker than in doped a-Si:H, so we can expect to have less interface defects when the hetero-interface is formed with undoped rather than doped a-Si:H. Fig. 4 shows the

ideal case (without considering the interface state density) simulations for the photovoltaic properties of the solar cells with the intrinsic layer thickness.

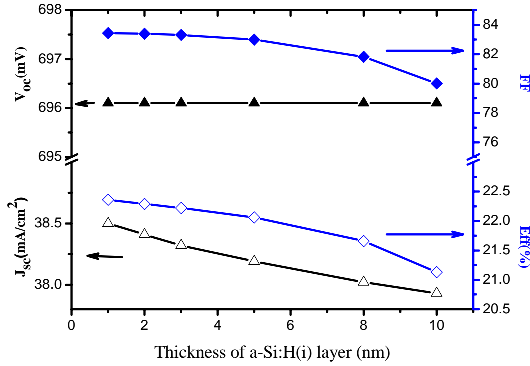

Fig. 4. The simulated parameters of the TCO/a-Si:H(p$^+$)/a-Si:H(i)/c-Si(n)/a-Si:H(n$^+$)/TCO solar cell versus the thickness of the embedded a-Si:H(i) layer.

It can be seen from Fig. 4, inserting a thin intrinsic layer can improve the efficiency, such as the introduction of the 1nm thickness intrinsic layer can increase the cell efficiency up to 22.36%. This is because that the a-Si:H layer insertion has an important advantage. Since the diffusion length of free carriers is short in the a-Si:H layer, the carrier drift by electric field is more effective than by diffusion. The thin a-Si:H (i) layer insertion can enhance the width of the depletion region in the two a-Si:H layers and increase the contribution of the drift current [2]。

However, with the increase of the intrinsic layer thickness, the fill factor and short circuit current of cell decline. When the intrinsic layer thickness exceeds 5nm, the conversion efficiency of solar cell with an intrinsic layer is even lower than the structure without the intrinsic layer. For when the intrinsic layer thickness increases, the short-wavelength illumination is mainly absorbed by the amorphous silicon layer, where the carrier mobility is much lower compared to the crystalline silicon. The corresponding photo-induced carriers could not be collected effectively, which deteriorate the short-wavelength response and the short-circuit current. In addition, the thicker intrinsic layer leads to increase of the series resistance, and series resistance is one important factor of the fill factor, causing the decrease of the fill factor [7]. Therefore, the introduction of the intrinsic layer should be used to reduce the influence of the interface states density and passivate the a-Si: H (p)/c-Si (n) hetero-junction. Taking into account the production processes, the thickness of the intrinsic buffer layer is set at 3nm.

3.1.3.2 The interface defect states without intrinsic layer were added.

The previous simulations are the ideal cases for solar cells, but in actual production, the impact of interface defect states can't be ignored. Fig. 5 shows the influence of the interface states density on the characteristics of the HIT solar cells. There is no intrinsic layer between the a-Si: H (p$^+$) layer and c-Si (n) layer here, whereas the interface defect states were added on the interface. The interface defect states density varies from 10^9-10^{14}cm^{-2}, with corresponding electron and hole capture cross section of donor states and acceptor states are 10^{-15}cm^2 ,10^{-17}cm^2, 10^{-17}cm^2 and 10^{-15} cm^2, respectively.

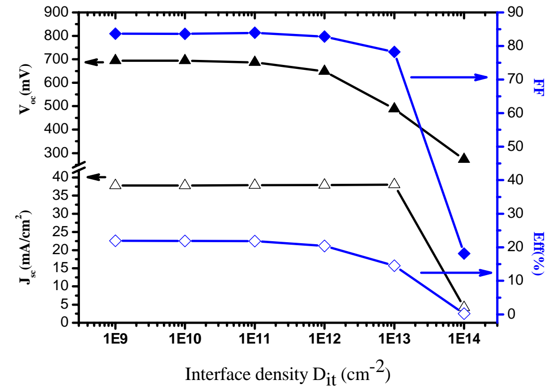

Fig. 5 The simulated parameters of the TCO/a-Si:H(p$^+$)/c-Si(n)/a-Si:H(n$^+$)/TCO solar cell versus the interface density D_{it} .

In Fig.5, we can see that when D_{it} <10^{11}cm^{-2}, the solar cell's performance are almost free from the influence of interface defect states; but when D_{it}> 10^{11}cm^{-2}, the cell performance decreases dramatically except the short-circuit current. Under the condition D_{it} = 10^{13}cm^{-2}, the open circuit voltage and conversion efficiency of the solar cell reduced to 488.3mV and 14.53%, respectively. This was mainly due to increase of the recombination happened in the depletion region, which was caused by the interface defect states. So the reverse leakage current of solar cell increases. According to the ideal diode model of solar cells, the relationship between the open circuit voltage and the reverse saturation current J_0 is as following:

$$V_{oc} = \frac{k_0 T}{q}[\ln(J_{sc}/J_0) + 1]$$

Moreover, a similar expression exists between the fill factor FF and J_0 when the series resistance can be ignored[8]：

$$FF \cong \left\{1-\frac{1}{\ln(J_{sc}/J_0)}\right\}\left\{1-\frac{\ln[\ln(J_{sc}/J_0)]}{\ln(J_{sc}/J_0)}\right\}$$

Therefore, the increase of J_0 will inevitably lead to the decrease of V_{oc} and FF, which reduces the efficiency of solar cells.

3.1.3.3 Both an intrinsic layer and the interface defect states are added.

Fig. 6 shows the influences of the intrinsic amorphous buffer layer thickness on the photovoltaic properties of solar cell under different interface defect states density. Usually the introduction of the amorphous buffer layer can reduce the interface states density, now the interface states density varies from 10^9 to $10^{12}cm^{-2}$. In Fig.6, we can see that the trends of all parameters are the same as discussed in section 3.1.3.1 and 3.1.3.2. With the increase of the intrinsic layer thickness, all photovoltaic parameters decrease except a tiny increment in short circuit current; and with increase of the interface states density, the similar decline happened for V_{oc}, FF and J_{sc}. It can be seen from the Fig.6, for solar cell with the thickness of intrinsic buffer layer less than 5nm, the interface defect states have little effect on the conversion efficiency if $D_{it}<10^{11}cm^{-2}$.

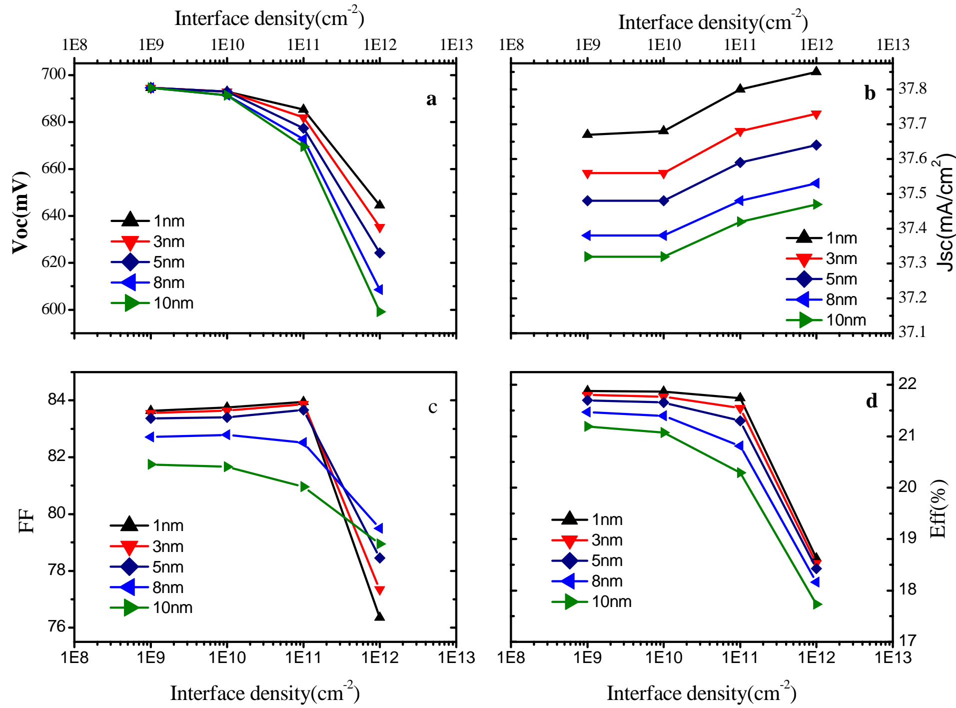

Fig. 6 The simulated parameters of the TCO/a-Si:H(p⁺)/a-Si:H(i)/c-Si(n)/a-Si:H(n⁺)/TCO solar cell as function of different intrinsic layer and the interface density D_{it} .

3.1.4 Influence of the front TCO/a-Si:H(p+) contact

Fig.7a shows the dependence of the TCO/a-Si:H(p^+)/a-Si:H(i)/c-Si(n)/a-Si:H(n^+)/TCO solar cell performance on variation of the work function W_{TCO}, The inserted a-Si:H(i) layer is 3nm and no interface density was included. The ITO work function varies from 4.3 to 5.1eV, depending on the stoichiometry and deposition method of the ITO layer [4].

From Fig.7a, with the work function W_{TCO} increases from 4.9eV to 5.1eV, faster growth in most parameters of the solar cell, then close to saturation. To understand this, it needs to take into account the energy band diagram shown in Fig. 7b, where the work function W_{TCO} is 4.9eV. It is evident that the TCO/a-Si:H(p^+) contact and the a-Si:H(p^+)/c-Si(n) junction locate on each side of the emitter, respectively. When W_{TCO} is low, the Fermi energy E_f of TCO is higher than that of a-Si:H(p^+), the V_D of the TCO/a-Si:H(p^+) contact have an inverted direction to that of the a-Si:H(p^+)/c-Si(n) junction, which decreases the V_{OC} and the FF. With the increase of W_{TCO}, V_D of the TCO/a-Si:H(p^+) contact decreases and the front contact is

near a flat band, so that the built-in voltage increases and results in a higher V_{oc}. Therefore, during the preparation of TCO film, it is necessary to consider the impact of the work function W_{TCO}. For the emitter with $2\times10^{19}cm^{-3}$ doping, the corresponding flat band work function is 5.27eV and at that time the cell efficiency is above 22%.

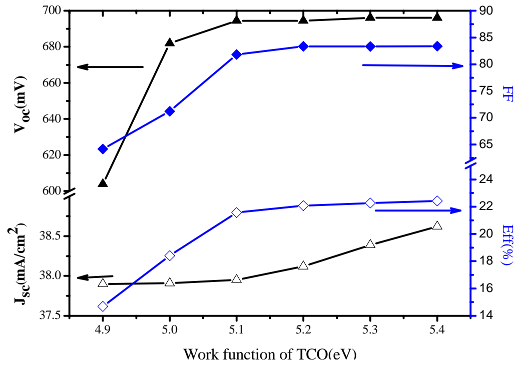

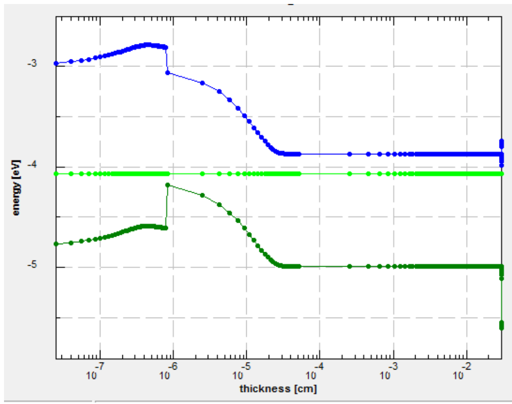

Fig. 7. a)The simulated performance of the TCO/a-Si:H(p$^+$)/a-Si:H(i)/c-Si(n)/a-Si:H(n$^+$)/TCO solar cell as a function of various W_{TCO}, the inserted a-Si:H (i) layer is 3nm. b)The band diagram of the TCO/a-Si:H(p$^+$)/a-Si:H(i)/c-Si(n)/a-Si:H(n$^+$)/TCO structure with W_{TCO}=4.9eV.

3.2 Optimization of the back stucture

3.2.1Optimization of the a-Si:H (n$^+$) doping concentration

Now the impact of back surface field (BSF) doping concentration on the solar cell is considered. The structure of the solar cell is TCO/a-Si:H(p$^+$)/a-Si:H(i)/c-Si(n)/a-Si:H(i)a-Si:H(n$^+$)/TCO with the assumption that the back contact is a flat band and no interface defect states was considered.

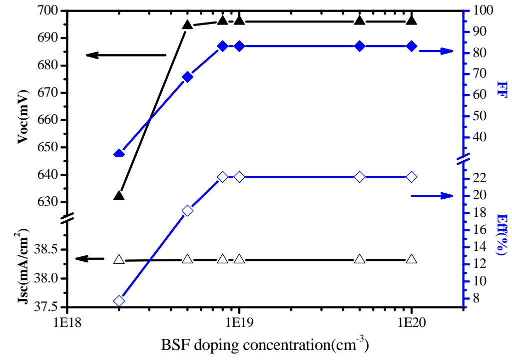

Fig. 8. The simulation results of TCO/a-Si:H(p$^+$)/a-Si:H(i)/c-Si(n)/a-Si:H(i)/a-Si:H(n$^+$)/TCO solar cell versus the BSF doping concentration.

In Fig. 8, with doping concentration increasing, in addition to short-circuit current is constant, the open circuit voltage, fill factor and efficiency gradually increase and then saturate. The simulation results show that N_D is required to be higher than $8\times10^{18}cm^{-3}$ in order to obtain good performance. This reason is attributed to the BSF band structure. When the BSF doping concentration is low, the reflection role of the BSF is not obvious, so the fill factor is low. The potential barrier for carrier transport can be reduced by increasing the doping concentration, which will reduce the barrier width and enhance the tunneling opportunity [9]. When the BSF doping concentration is higher than the substrate doping concentration about two magnitudes, a good BSF is formed. With the doping concentration further increases, this effect is saturated. In our simulation, the BSF doping concentration is selected as $1\times10^{19}cm^{-3}$.

3.2.2 Influence of the back TCO/a-Si:H(n$^+$) contact

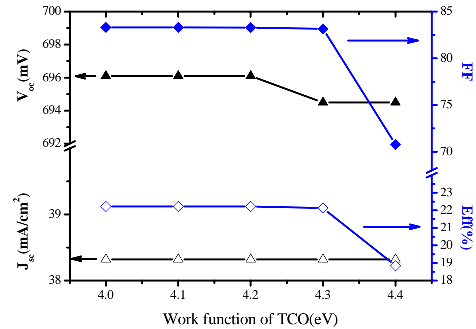

Fig. 9 The simulated parameters of the TCO/a-Si:H(p$^+$)/a-Si:H(i)/c-Si(n)/a-Si:H(i)/a-Si:H(n$^+$)/TCO solar cell as a function of back contact work function W_{TCO}.

Fig. 9 shows the dependence of the TCO/a-Si:H(p^+)/a-Si:H(i)/c-Si(n)/ a-Si:H(i)/a-Si:H(n^+)/TCO solar cell performance on the back TCO work function W_{TCO}. The BSF doping concentration is $1\times10^{19}cm^{-3}$, corresponding to the flat work function W_{TCO} is 4.06eV. The computation results show that a higher value of W_{TCO} will make the solar cell performance inferior. This behavior is similar with the case which was discussed in section 3.1.4, so there is no necessary to discuss again here.

3.3 Influence of the interface defect states

In order to understand the effect of the interface defect states, we simulated the solar cell structures show in Fig.1 for obtaining their J_{sc}, V_{oc}, FF and efficiency (Eff), as a function of the total interface defect states density D_{it}. Fig. 10a shows the results for the HIT structure with an intrinsic a-Si layer and Fig. 10b gives the results for solar cell structure without an intrinsic a-Si layer.

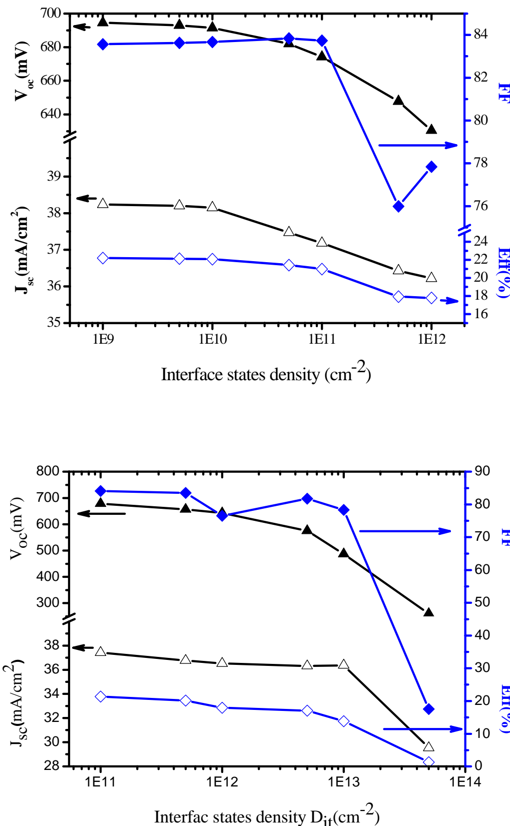

Fig. 10a Results for the HIT structure with an intrinsic a-Si layer versus D_{it}. b Simulation results for the HIT structure without a-Si layer versus D_{it}.

In both figures we observe a declining efficiency when the density of interface defect states increases. An important result shown in these figures is the fact that if we can control the interface states density less than $1\times10^{11}cm^{-2}$, the efficiency around 21% can be reached in the case of the structure without intrinsic a-Si layer, which is just one percent lower compared to standard HIT solar cell. This further confirms our judgment that the inserted intrinsic layer is mainly used to suppress the interface defect states and passivate the doped a-Si:H/c-Si interface. In other words, the intrinsic layer can be cancelled if the hetero-junction interface is low defect states density.

4. Conclusions

The performance of bifacial TCO/a-Si:H(p^+)/a-Si:H(i)/c-Si(n)/a-Si:H(i)/a-Si:H(n^+)/TCO solar cell was investigated by using the AFORS-HET software. The influence of various parameters for the front and the back structures were studied. The computation results shows that for the front TCO/a-Si:H(p^+)/a-Si:H(i)/c-Si(n) contact, the optimal doping concentration and thickness of emitter are $2\times10^{19}cm^{-3}$ and 5nm, respectively. A 3nm a-Si:H(i) layer is suitable for embedding between a-Si:H(p^+)/c-Si(n). For the back c-Si(n)/a-Si:H(i)/a-Si:H(n^+)/TCO contact, W_{TCO} should be as low as possible and the BSF doping concentration should be higher than the base doping concentration about two magnitudes. The high interface defect states on a-Si:H(p^+)/c-Si(n) interface and c-Si(n)/a-Si:H(n^+) interface will deteriorate the hetero-junction solar cell performance, so an intrinsic buffer layer should be introduced to suppress the interface density.

Acknowledgements

This paper is supported by “The Fundamental Research Funds for the Central Universities”(Project number:2010-la-019),

References

[1] J. P. Kleider, R. Chouffot, A. S. Gudovskikh, P. R. Cabarrocas, M. Labrune, Thin Solid Films **517**, 6386(2009).
[2] L. Zhao, C. L. Zhou, H. L.Li, H. W. Diao, W. J. Wang Solar Energy Materials & Solar cells. **92,** 673(2008).
[3] W. Fuhs, L. Korte, M. Schimidt. J. Optoelectron. Adv. Mater., **8**, 1989 (2006).
[4] H. C. Norberto, M. A. Arturo, Solar Energy Materials & Solar cells, **94,** 62 (2010).
[5] Lin Hongsheng, Ma Lei, Research & Progress of SSE, **23**, 470 (2003).

[6] M. Schmidt, L. Korte, A. Laades, R. Stangl, Ch. Schubert, H. Angermann, E. Conrad, K. V. Maydell, Thin Solid Films **515**, 7453(2007).
[7] B. Y. Ren, Y. Zhang, B. Guo, B. Zhang, H. Y. Li, Y. Xu, W. Wang, J. Acta Energy Solaris Sinica **29**, 1112(2008).
[8] Hu Zhi-hua, Liao Xian-bo, Zeng Xiang-bo, Xu Yan-yue, Zhang Shi-bin, Diao Hong-wei, Kong Guang-lin. Acta Physica Sinica, **52**, 217(2003).
[9] L. M. Li, B. Q. Zhou, X. Chen, B. Han, L. Y. Hao, Information Recording Materials, **10**, 18(2009).

*Corresponding author: wang_lesson@yahoo.com.cn